USING THE HART II DATA BASE TO IMPROVE BVI NOISE PREDICTION

Guillaume Perez* and Joëlle Bailly**

* ONERA / Department of Acoustics Numerical Simulations
Châtillon, France
e-mail : guillaume.perez@onera.fr

** ONERA / Department of Applied Aerodynamics
Châtillon, France
e-mail : joelle.zibi@onera.fr

Key words: BVI noise prediction, empirical models, core radius, velocity profile, free wake

Abstract. The current paper demonstrates how the more precise knowledge of the rotor wake characteristics obtained with modern wind tunnel tests can be used to improve BVI noise prediction. New empirical laws describing the vortex and its aging are derived from experimental data. The impact of these vortex description improvements on noise prediction is assessed. The second issue under examination is the importance of a roll up model inclusion in the free wake computation. This concept is evaluated in the light of HART II experimental results.

INTRODUCTION

Over the past twenty years extensive studies have been performed to predict BVI noise. In this process two different approaches were followed. The first one based on the accurate prediction of the wake aerodynamics through the use of CFD still remains challenging. Although recent progresses have been made[1,2,3], the physical dimensions of the rotorcraft problem still render difficult a fine description of the vortex (number of grid points representing its core), which leads to vortex diffusion rates greater than the one experimentally observed. The other method has consisted in simplifying the wake description, by discretizing it in vortex segments or panels [4,5], in order to compute more easily its evolution. These simpler methods required the use of physical models [6,7] to take into account complex wake features they could not predict such as the vortex sheet roll up or the aging of the resulting vortices. These models were based on wind tunnel test observations, but until recently the flow visualization techniques could not capture the vortex characteristics with the accuracy needed by computation codes. This paper will present how these models (implemented in the ONERA computation chain) and thus BVI noise prediction can be ameliorated by using the results of a modern and highly instrumented wind tunnel test such as HART II [8, 9].

The first part of the article will briefly describe the ONERA computation chain [10,11]. In this description we will outline which parameters are issued from empirical laws and how these laws can be improved based on HART II results. In a second part, we will examine the relevant test data and derive new versions of the models from this analysis. The impact of these modifications on noise prediction will be assessed. Eventually we will take advantage of another output of HART II, the precise knowledge of the wake geometry, to evaluate the importance of the roll up model inclusion in the free wake computation. This concept, consisting in putting at equilibrium a concentrated vortex sheet rather than a distributed one, is thought to better represent the kinematics of the wake. The impact of this concept on the predicted wake geometry and noise will be thoroughly examined.

CODE AND MODEL DESCRIPTION

In this paragraph the architecture of the ONERA BVI noise computation chain is briefly recalled (Figure 1). The different physical models present in the codes are described and their potential betterment using HART II data is discussed.

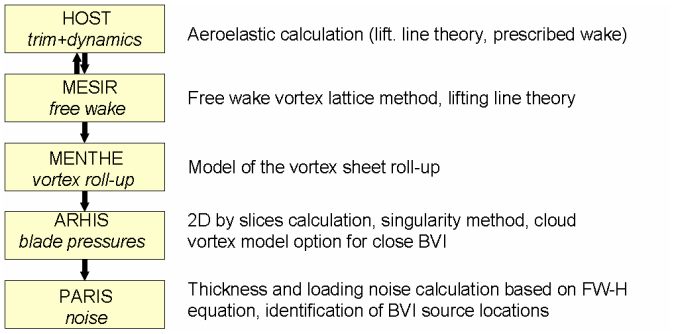

Figure 1: Architecture of BVI noise prediction chain

The HOST and MESIR [6] codes which are coupled compute the dynamics of the rotor and the wake geometry. Then MENTHE [7] concentrates the vortex lattice issued from the free wake computation to generate the interacting vortices. The aerodynamics of the interaction is determined by ARHIS [12] providing thus blade pressures to the acoustic code PARIS for BVI noise prediction.

The totality of the empirical models describing the wake and tip vortex evolution is comprised in MENTHE and ARHIS. MENTHE characterizes the roll up phase. At each azimuth, it determines the number of vortices that are generated by the blade and their circulation. The laws representing the vortex sheet roll up were obtained from HART I [13,14] and a former test campaign [18]. Both wind tunnel tests used Laser Doppler Velocimetry (LDV) to measure the evolution of the tip vortices. In these experiments, LDV enabled to obtain the vortex circulation with a good accuracy. Although the Particle Image Velocimetry (PIV) realised in HART II [15] gave us more accurate results concerning the details of the vortex structure (core radius, shape of the velocity profile), it is not thought to significantly improve the determination of vortex circulations. Since MENTHE empirical laws only deal with this vortex parameter we saw no need to modify the roll up models by using HART II data.

In order to compute the aerodynamics of BVI, ARHIS necessitates the precise knowledge of the vortex characteristics at the interaction age. Key vortex parameters driving the interaction are the core radius and the velocity profile. Actually they contribute to determine the impulsivity and intensity of the BVI phenomenon. Since these parameters cannot be computed directly from the first principles in a comprehensive analysis approach, they have to be modelled by empirical laws. The presence, in the HART II test, of numerous PIV measurement planes along the vortex paths enables to have a fine representation of the vortices and to observe their evolution with respect to time. This detailed knowledge of the vortex structure and its evolution through time was not accessible in former experiments. That is why we expect a noticeable amelioration of ARHIS vortex models thanks to HART II data, which should lead to a more precise prediction of the blade pressure fluctuations created by BVI. Let us now describe how these models are implemented in ARHIS and how they can be modified. During the interaction the vortex is represented by a cloud of vorticity disks (Figure 2). The size of each vorticity disk is parametrable and is made to follow an “aging” law depending on the vortex total circulation. The core radius evolution is thus easily modifiable since it explicitly depends on an analytical expression programmed in the code. The modification of the velocity profile is less straightforward. Each vorticity disk carries a fraction of the total circulation of the vortex. By changing the repartition of circulation between the different layers of disks, one can modify the profile of induced velocity. Figure 3 illustrates how different shapes of velocity profiles can be obtained following this method. An iterative process will be necessary to find a circulation distribution enabling to match HART II vortex velocity fields.

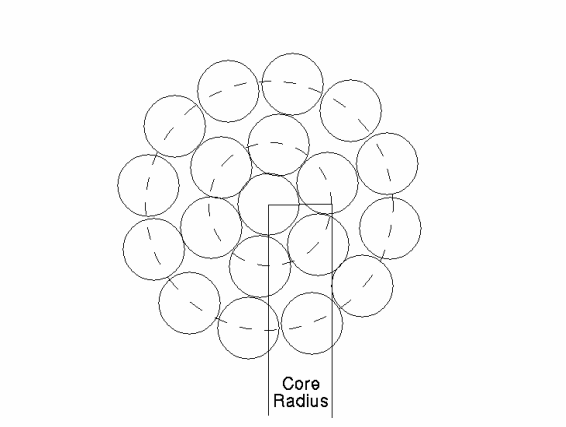

Figure 2: Vortex representation in ARHIS (the number of vorticity disks and vorticity disk layers is not representative)

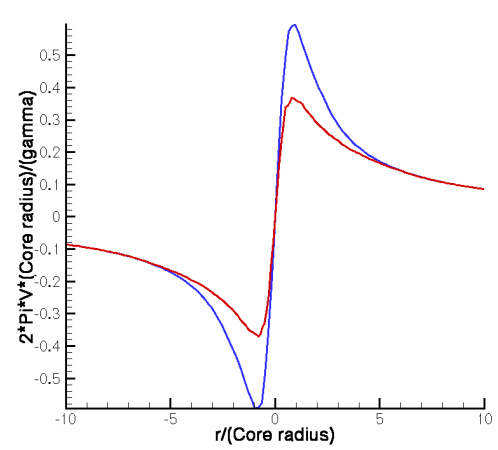

Figure 3: Example of velocity profiles obtained in ARHIS.

IMPROVEMENT OF PHYSICAL MODELS

In this section, we will not describe in details how the experimental results concerning the evolution of the core radius and the velocity profiles were obtained. Several articles have thoroughly presented the HART II test set up [8,9] and the proper analysis methodologies [11,16,17]. We will simply recall the main principles of the vortex characteristic derivation.

The test case chosen to adjust our models is the baseline configuration. Actually the corresponding flight conditions (descent angle=-6°, $\mu = 0.15$) are prone to generate BVI and the characteristics of the interacting vortices are thought to be representative of the whole BVI domain. We also chose this test case because no High Harmonic Control (HHC) was applied. Such a device affects the spanwise distribution of blade circulations and thus can artificially modify the attributes of the generated vortices.

Core radius evolution law

As mentioned before, the presence of numerous high resolution PIV planes (Figure 4) along the vortex paths enables to study the evolution of their structure through time.

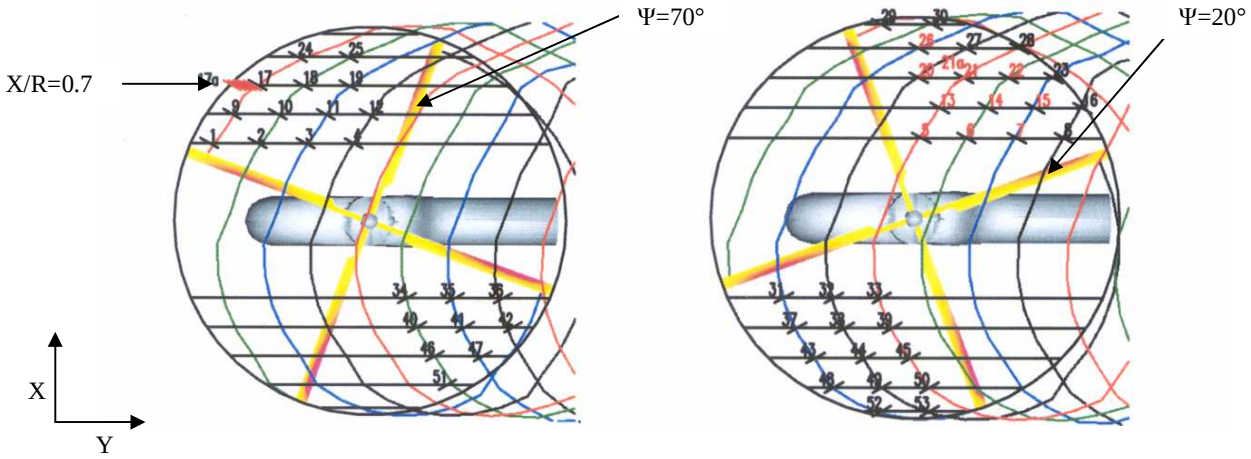

Figure 4: Position of PIV measurement planes

To determine the law characterizing the vortex core growth, the $X/R = 0.7$ measurement line was chosen. The vortex following this path interacts with the blade section situated at $0.9R$ (the interaction azimuth being 50° in this flight configuration). This outboard section is in the blade spanwise range generating the more intense noise, thus the vortex captured in this measurement line is representative of the interacting vortices which we aim at modelling.

For each PIV plane, conditional averaged vorticity maps are derived from the 100 instantaneous measured velocity fields. The conditional average is necessary to eliminate the model movements and the vortex wander, in order to determine the vortex characteristics (core radius and peak swirl velocity) in an accurate way. These vorticity fields are reoriented in order to take into account the fact that the vortex axis is not orthogonal to the measurement plane, as illustrated in Figure 5 by a well-defined circular vorticity distribution.

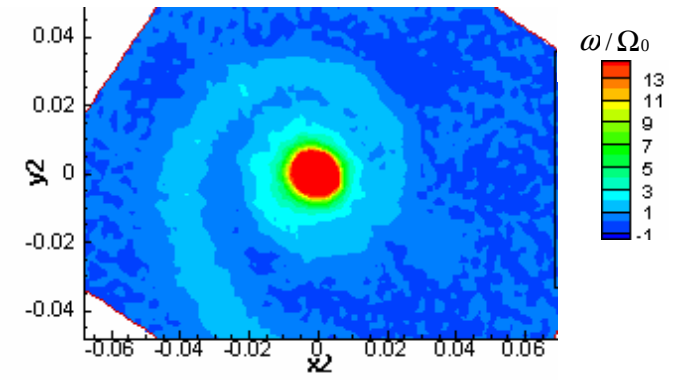

Figure 5: Averaged vorticity field obtained after the reorientation process (Ω_0 being the rotation speed of the rotor).

From this averaged field, the circulation is computed as a function of the distance to the vortex centre and consequently the profile of swirl velocity $v_\theta(r) = \Gamma(r)/(2\pi r)$ can be determined. At this stage, the core radius is readily deduced from the velocity profile (radius for which the maximum value of swirl velocity is obtained). Figure 6 presents the evolution of the vortex core radius obtained through this process. The same analysis was conducted on the retreating side but the corresponding results are not presented here for concision reasons.

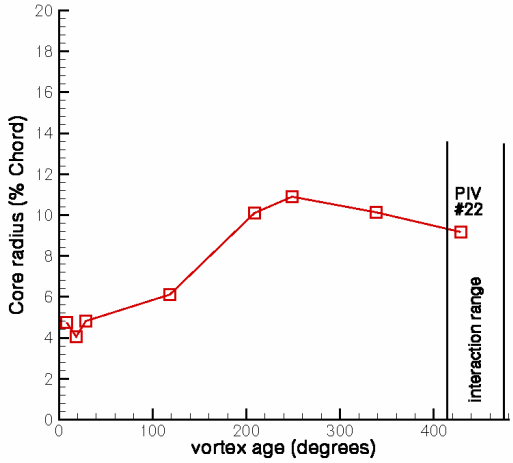

Figure 6: Experimental evolution of the vortex core radius with respect to vortex age.

In the ARHIS code, two phases are distinguished. The vortex evolution starts with a roll up phase where the vortex grows both in terms of core size and circulation. Then follows a diffusion phase where the viscous core pursues its growth while its circulation remains constant. Due to the lack of exploitable data concerning the vortex evolution in HART I, the vortex diffusion phase was modelled by a simple linear law which conducted to unrealistic diffusion at high ages. The extent of the HART II data base enabled us to have a more precise model following the theoretical turbulent diffusion of the vortex. The size of the core radius evolving according to the expression: $Rc(t) \approx K\sqrt{\nu_T * t + r_0^2}$. A simple dimensional analysis links the turbulent eddy viscosity ν_T to the vortex circulation. On the aerodynamics point of view this hypothesis is equivalent to assuming a fully turbulent vortex peripheral flow. Although the vortex peripheral flow is in a transitional state [19], this hypothesis should lead to an acceptable first order prediction of the vortex diffusion phenomenon. The model constants (K and r_0) were chosen to minimize the difference between the predicted core size and the measured one for both the advancing and retreating side. Figure 7 compares the former and new models to experimental data on the advancing side. It was chosen to present the corresponding core size evolutions in the vortex model time base [20] which serves as a common time base.

As it can be seen, the new model brings a clear improvement concerning vortex diffusion, the new diffusion rate being closer to the one experimentally observed.

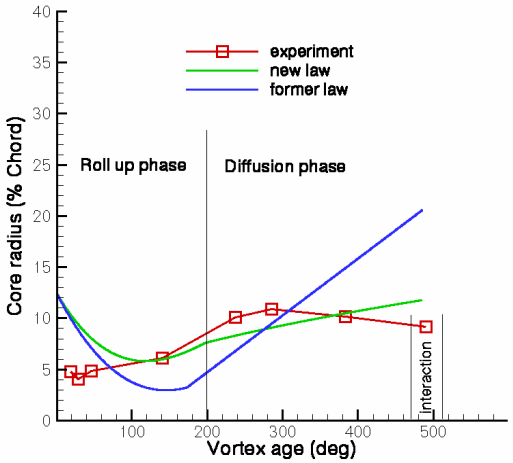

Figure 7: Improvement of core size prediction.(Data presented in the vortex model time base)

Concerning the roll up phase, one may be surprised by the initial decrease (in the computation) of the core size which does not correspond to any physical phenomenon. In fact, the viscous core size starts from a relatively high value in ARHIS to counterbalance the fact that the circulation is constant in the code, which does not fit the vortex evolution physics. In reality, if an interaction occurred at very early ages, the blade response would be rather low because the vortex circulation would be weak since the wake is in the beginning of the roll up phase. This numerical artefact consisting in increasing the vortex core size while keeping the final value of circulation enables to reproduce a similar blade aerodynamic response.

Velocity profile

The derivation of the vortex velocity profiles is outside the scope of the present paper. In this paragraph we will simply recall one of the findings concerning the vortex characteristics in descent. The vortices generated in advancing flight conditions are much weaker than the one generally observed in hover [17]. Such differences are not surprising since the spanwise repartition of circulation in advancing flight is substantially different from the one observed in hover. For the reasons stated in the previous section, we used the baseline case data to tune our

velocity profile model. We considered the PIV plane n° 22 (Figure 4) because the corresponding vortex age is very close to the age of interaction. Figure 8 presents the averaged velocity field induced by the vortex.

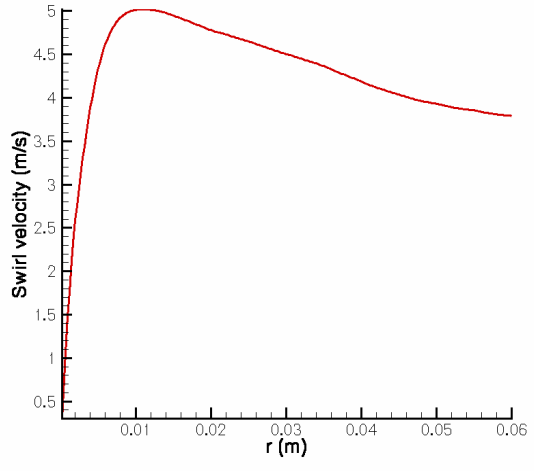

Figure 8: Induced velocity with respect to the distance to the vortex centre (cut 22)

The maximum induced velocity is rather low ($V_{\max} \approx 0.25 \times \Gamma/(2\pi \times R_c)$, Γ: vortex circulation, R_c: core radius). As a matter of comparison, a "Scully" theoretical vortex of same circulation would induce a maximum velocity twice greater. It can also be noticed that the velocity decreases slowly as a function of the distance to the vortex centre. This velocity plateau denotes that the vortex vorticity is distributed over a large area. It is an important feature for BVI prediction. Actually this vortex characteristic will lead to a slower decrease of the aerodynamic blade response with respect to the miss distance.

As mentioned in the first part of this article the vortex representation in ARHIS allows the modification of the vorticity distribution inside the vortex. Experientially we obtained a distribution producing a relatively slow decrease of induced velocities as a function of the distance. As it can be seen in Figure 9 this new velocity profile model brings a significant improvement for the prediction of vortex induced velocities at relatively large distances from the core.

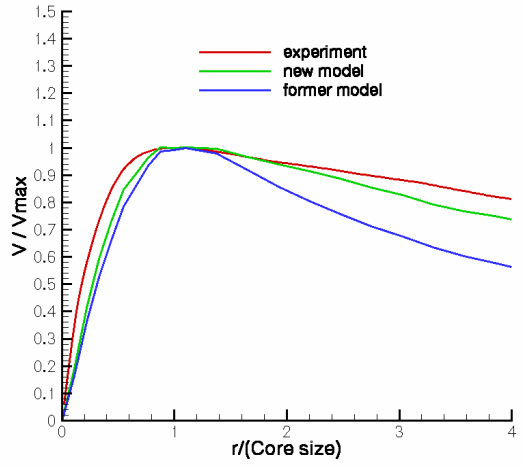

Figure 9: Improvement of induced velocity model. Comparison of former and new models to experiment.

Impact of model improvements on noise prediction

In order to see the importance of these vortex characteristics (core radius, velocity profile) on BVI noise, and to assess the gains obtained with the new models, acoustic computations were performed with former and modified empirical laws. To get rid of the uncertainty concerning the miss distance, another key parameter driving BVI, the wake was displaced to match experimental positions for both computations. Figure 10 demonstrates that the vortex characteristics have a significant impact on noise. The passage from the first empirical laws to the new ones increased the computed maximum level of noise by 2.8 dB and reduces the discrepancy with experimental data.

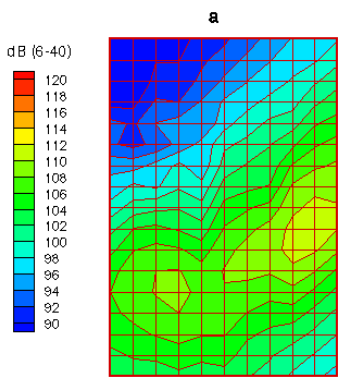

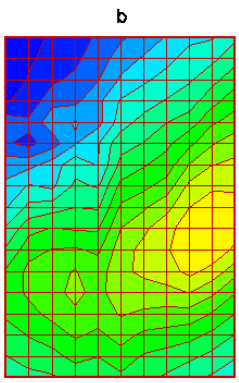

Figure 10 a,b: HART II Baseline case. Computed noise footprints with:
a) previous models
b) new models

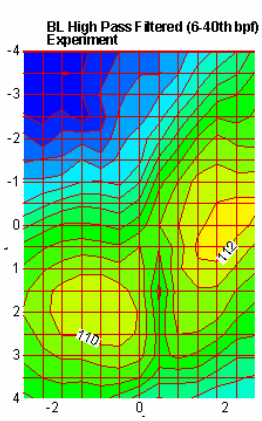

Figure 10 c: Measured noise footprint

CONCEPT EVALUATION USING HART II

In this last part, the inclusion of a roll up model in the free wake computation is evaluated. This concept was implemented because it was considered that the kinematics of a rolled up wake could differ from the kinematics of a distributed one and would represent better the physics of the phenomenon. The potential ameliorations concerning the wake geometry prediction are assessed and their effects on noise prediction are determined on the three HART II main cases, namely the baseline, minimum noise and minimum vibration cases.

Concept explanation

Let us describe first the main principles of the MESIR [6] free wake computation. The blade aerodynamics is computed using a lifting line theory. The wake is described by a vortex lattice composed of tangential and radial vortex filaments. The tangential filaments represent the spanwise variations of circulation and the radial ones represent the variation of circulation through time. A first computation of the wake is done by considering a prescribed helicoïdal geometry. This geometry is obtained using the Meijer-Drees formula. Then this prescribed wake is distorted using a free wake analysis. Several iterations of the distortion process are necessary to reach a stable wake configuration. Between iterations the circulations on the blade are recomputed. A relaxation algorithm enables to obtain converged circulations corresponding to each intermediate wake geometry.

It was decided to introduce the roll up once the distributed wake has reached equilibrium. At this stage, using the method implemented in MENTHE (described in details in [7]), we determine which tangential vortex

filaments will be included in the concentrated vortices (corresponding to the physical wake roll ups). Then these tangential filaments are progressively brought closer toward their barycentre. This process takes place when the age of the vortex segments is bounded by 50 and 100 degrees (Figure 10).

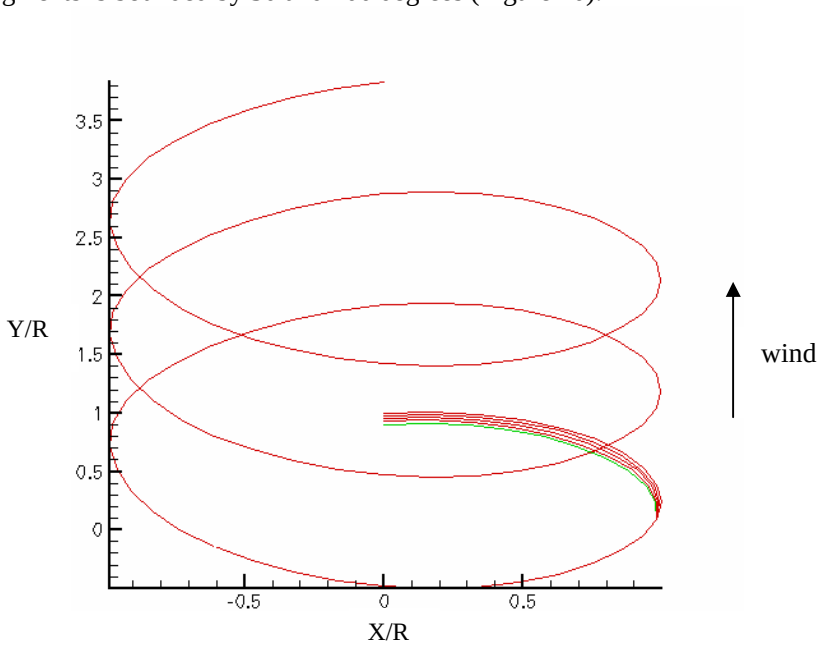

Figure 10: Top view of the wake: illustration of initial the roll up process.

After this period all the filaments participating in the roll up have merged, which is consistent with the experiment. Actually the study of the evolution of the tip vortex circulation with respect to time in a former test campaign [18] shows that circulation reaches its maximum value at an age of approximately 100 degrees. Furthermore, we have chosen not to modify the position of the vortex filaments until the age of 50 degrees because the close wake has an important influence on the blade loads. Doing so, we insure that the roll up process does not alter the computation of the blade loads (especially their spanwise distribution).
Once the wake is concentrated, several deformation iterations are necessary to put this rolled up wake at equilibrium. Between these iterations, the circulations on the blade are recomputed in order to have blade loads consistent with the wake geometry.

Let us discuss the consequences of the procedure described above on the radial vortices and their induced velocity fields. Actually, once the tangential filaments have merged, the radial vortices situated between those filaments have seen their length reduced to zero. In this case, the velocity field given by the discretized form of the Biot and Savart law (see below) is not defined.

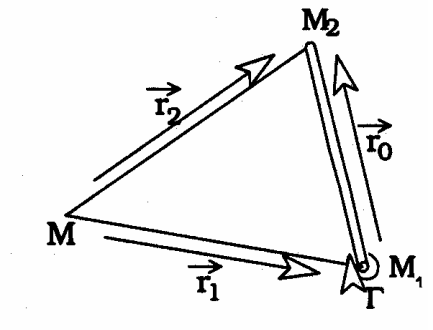

Velocity induced at the point M by the vortex segment M1M2:

$$\vec{V}_i = \frac{\Gamma}{4\pi} * \frac{\vec{r}_0 \wedge \vec{r}_1}{\left\|\vec{r}_0 \wedge \vec{r}_1\right\|^2} . \vec{r}_0 . \left(\frac{\vec{r}_2}{r_2} - \frac{\vec{r}_1}{r_1} \right)$$

The regularization technique used in MESIR solves this problem. When the length r_0 of the vortex segment is equal to zero the velocity induced by this segment is null. We consider that the induced velocity of these radial segments being reduced to zero has no noticeable impact on the wake. Actually the blade loads present a rather low non steadiness due to the large time step used in the computation (typically 10°). As a consequence the circulation of the radial segments is rather small compared to the longitudinal segment circulations and their influence can be neglected.

Evaluation on the baseline case

The new version of the free wake code called MESIR RU was then tested on the HART II baseline case. Before analysing the wake geometry, it is necessary to verify that the inclusion of the roll up model has not altered the convergence process. As it can be seen on Figure 11, the wake has fully converged after 16 iterations of the deformation process. The main roll up, corresponding to the tip vortex that will cause BVI, is stable between the two last iterations of the free wake computation.

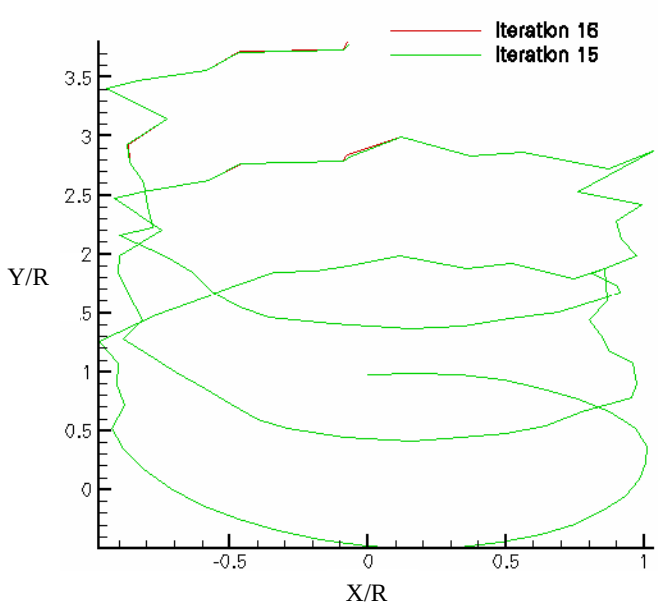

Figure 11: Convergence of the main roll up position (top view)

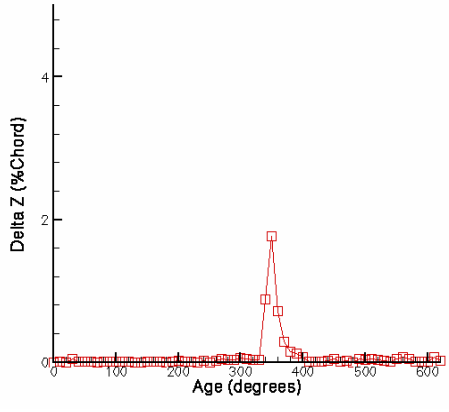

Figure 12: Difference of the roll up vertical position between the two last iterations. (wrt. age)

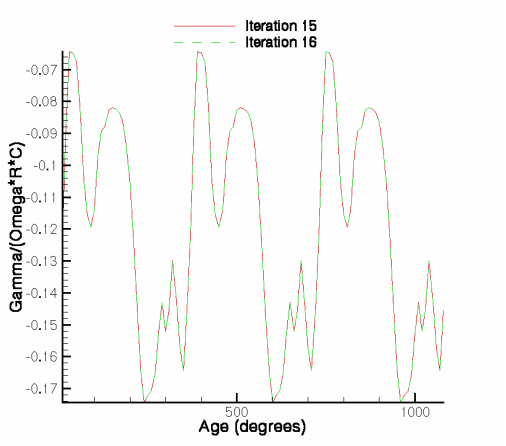

Figure 13: Comparison of circulation of the main roll up between the two last iterations. (wrt. age)

The mean difference between the vertical position of the roll up computed at iteration 15 and 16 was inferior to 0.5 % C (chord length). The maximum value of this difference does not exceed 2% C (Figure 12), which is deemed acceptable. Concerning the convergence of the roll up circulation, the mean difference between the two last iterations is less than 0.1% (Figure 13).

Once verified that the rolled up wake has reached a stable configuration in MESIR RU, we can assess the concept interest by comparing the new wake geometry to the one obtained with the former version of the code MESIR (Figure 14).

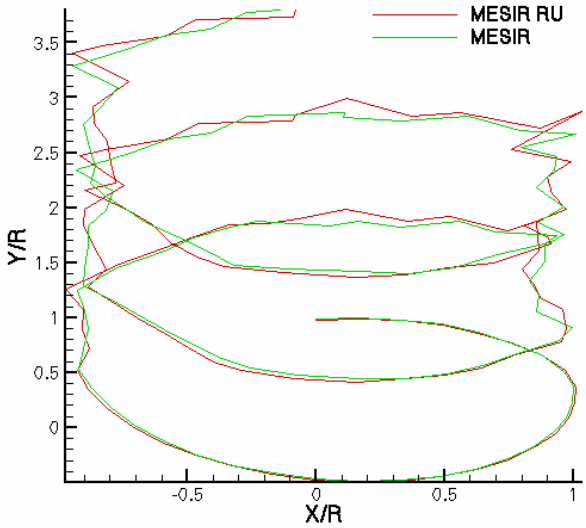

Figure 14: Top views of the rolled up vortex geometries obtained with MESIR and MESIR RU.

We can observe that the introduction of a roll up model modifies significantly the geometry of the wake. Both the position and the orientation of the main roll up have changed in a non negligible manner. Let us consider now the evolution of the vertical position of the wake which has a more direct impact on BVI. Figure 15 compares the vertical positions computed with the two versions of the code to experimental data obtained by PIV. The comparison between experiment and computations were made at the X/R=0.7R measurement line (advancing side fig 4.) and X/R=-0.7R (retreating side). (The X-axis sign convention is different between fig 4. and fig 14.)

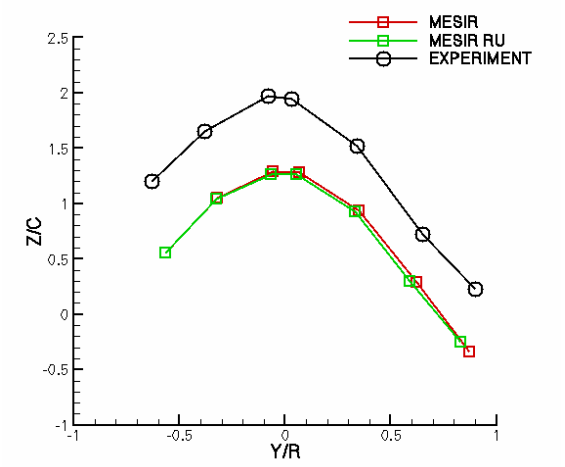

Figure 15 a: Side view of the wake: advancing side. Comparison of new and former computations.

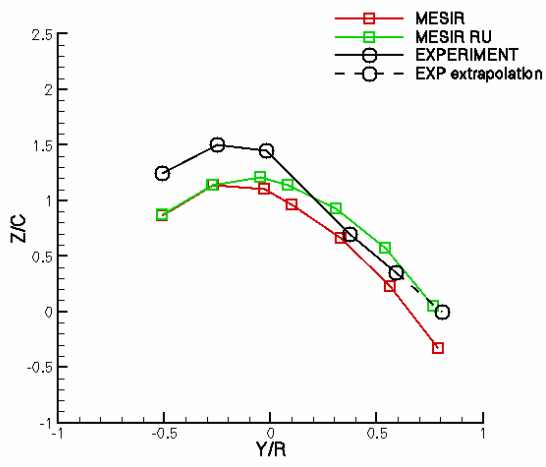

Figure 15 b: Side view of the wake: retreating side. Comparison of new and former computations.

One can observe that the geometries obtained with MESIR and MESIR RU are very close in terms of vertical positions for the advancing side. The maximum difference does not exceed 7% C. If we take a closer look at the zone where BVI occurs (Y>0.5R corresponding to $\Psi \in [40°,55°]$), we can notice that the vertical distance between the vortices generated by two successive blades is smaller in the MESIR RU computation than in the computation realised with MESIR (55%C compared to 65%C). Concerning this particular issue the geometry computed with MESIR RU presents a slight improvement in terms of correlation with experimental data. On the retreating side, we can observe that the two computed geometries are significantly different. The maximum vertical gap reaches 35 % C. In order to be able to determine which geometry will give a better BVI prediction, we had to extrapolate the experimental data. Actually BVI occurs in the ($Y>0.5R, \Psi \in [-55°,-40°]$) zone and experimental data was not available for Y>0.6R. In this zone, MESIR RU provides an enhanced geometry prediction. Thus one can expect an improvement concerning the BVI prediction for the retreating side with MESIR RU.

Let us see now how these differences in wake geometries affect BVI noise prediction. Figure 16 compares the two noise computations to the experiment. The noise levels are expressed in dB filtered between 6 and 40 bpf (blade passage frequency) in order to eliminate the low frequency loading noise and retain only BVI events. The two computations are very close concerning the prediction of BVI on the advancing side. In this region, the maximum noise level as well as the directivity are similar. However one can notice a slight broadening of the maximum noise region with the MESIR RU wake, which is consistent with the reduction of the distance between the tip vortices generated by successive blades observed in Figure 15-a.

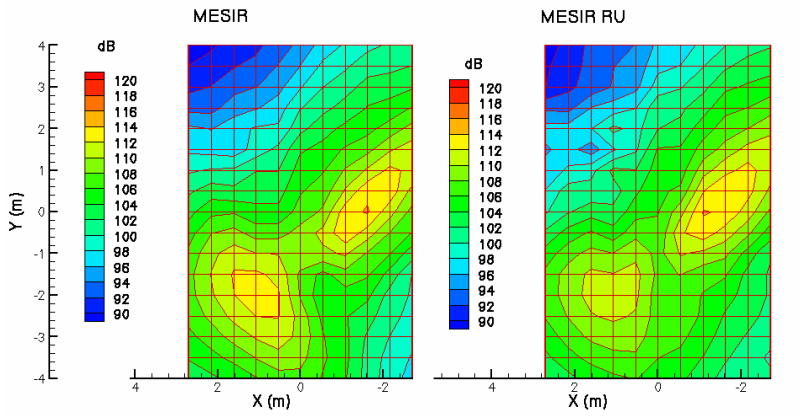

Figure 16 a: HART II Baseline case. Comparison of noise footprints obtained with MESIR (left) and MESIR RU (right)

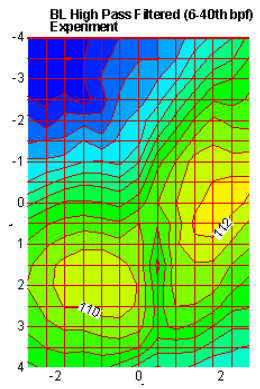

Figure 16 b: HART II Baseline case. Measured noise footprint

Concerning the retreating side, we observe significant prediction amelioration in terms of levels and directivity with the MESIR RU wake. The shape of the maximum noise region on the retreating side coincides better with the experiment, which means that the conformation of the interaction (vortex age, miss-distance, orientation of the vortex wrt. blade) is closer to reality. This is consistent with the wake geometry analysis performed in the previous paragraph.

Evaluation on the Minimum Noise case

This case corresponds to the same descent conditions as the baseline configuration but High Harmonic Control was applied with the intent to reduce BVI noise. The denomination, Minimum Noise case, corresponds to the best set of HHC parameters realizing this objective. In this configuration the modifications of blade loadings, introduced by HHC, lead to the creation of a second roll up at certain azimuths. A complete analysis of the rolled up wake convergence will not be performed for this case, however it can be noticed that the presence of a second roll up did not perturb the convergence of the free wake process. Actually the mean difference of the roll up vertical position did not exceed 1 % C between the two last iterations.

To evaluate MESIR RU, the vertical position of the wake is first considered. The vertical positions computed by the two versions of the code are compared to experimental data obtained by PIV. The comparison between experiment and computations were made at the same measurement lines as the one used in the previous section. Figure 17 shows that for the advancing side the wake geometries predicted by the two versions of MESIR are very close. The maximum gap represents 13% C. The differences are more significant concerning the retreating side. The difference between the two geometries reaches 32% C. However, if we restrain our study to the zone in which the interaction will occur ($Y/R \in [0.3,0.55], \Psi \in [-65°,-50°]$ in this case), despite this rather important gap we cannot conclude that a wake geometry is better than the other in terms of correlation with the experiment. In this zone it can also be noticed that, in both computations, the distance between the vortices generated by two successive blades is much smaller than the measured distance. This means that we will capture two strong interactions instead of one. In both computations we will probably overestimate the maximum noise level for the retreating side and the maximum noise zone will be larger in our computations than in the measured noise footprint.
At this stage of the analysis, we cannot conclude that the use of a roll up model in MESIR improves the accuracy of the wake geometry computation for the minimum noise case.

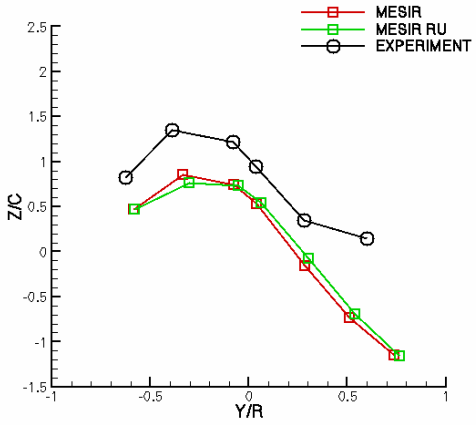

Figure 17 a: Main roll up vertical position: advancing side. Comparison of new and former computations.

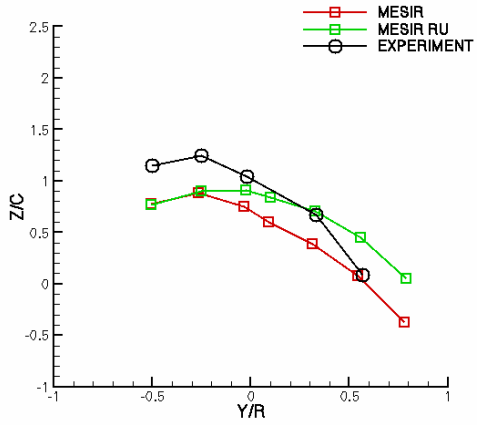

Figure 17 b: Main roll up vertical position: retreating side. Comparison of new and former computations.

Let us compare now the noise footprints obtained with two wake geometries computed with the different versions of the free wake code. Figure 18 compares the two computations to the experiment. Concerning the advancing side, the experimental footprint exhibits a large maximum noise zone which corresponds to two "close" interactions (in terms of miss distance) with vortices engendered by two successive blades. The prior computation (MESIR) underestimates the second interaction occurring at a higher azimuth. The use of MESIR RU leads to a more realistic prediction of the directivity because, in this computation, the second interaction is captured. This directivity improvement cannot be explained by a more accurate determination of the miss distance as it has been seen with the analysis of Figure 17-a. It is due to a better orientation of the roll up with respect to the blade. Actually in the MESIR RU computation the wake is situated higher than in MESIR. As a consequence the interaction with the blade happens earlier in terms of azimuth and thus the vortex is more parallel to the blade (the interaction angle is reduced by 5° in X-Y plane), which will increase the intensity of this BVI event. This modification of the wake geometry reduces the discrepancy with the measurements since the interaction also happens earlier in terms of azimuth in the experiment.

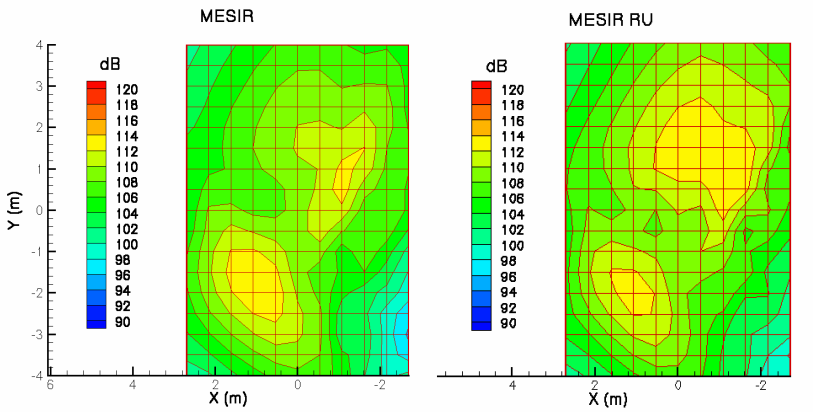

Figure 18 a: HART II Minimum Noise case. Comparison of noise footprints obtained with MESIR (left) and MESIR RU (right).

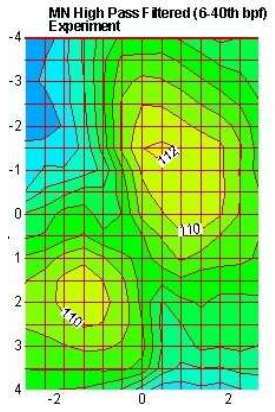

Figure 18 b: HART II Minimum Noise case. Measured noise footprint

Figure 19 presents the spanwise evolution of the miss distance for each vortex interacting with the blade. The increased intensity of the second BVI event can also be explained by a reduced interaction angle in the "Z-r plane" (the vortex corresponding to the second interaction is identified by the yellow colour in Figure 19). Specific experimental data is not available on this issue, but since the strength of the second interaction seems to be correctly captured in the MESIR RU computation, we can assume that the vortex obliquity is closer to reality in the new wake geometry.

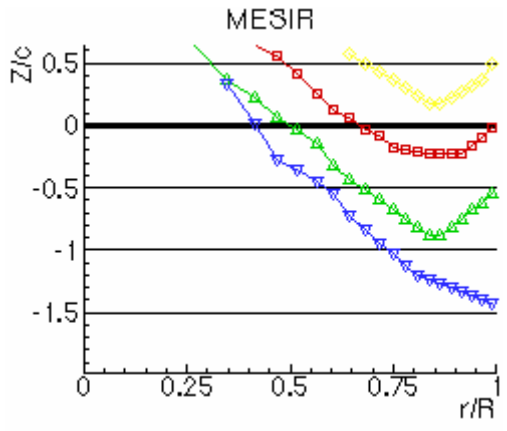

Figure 19 a: Visualization of interaction obliquities in the Z-r plane. (computation performed with MESIR)

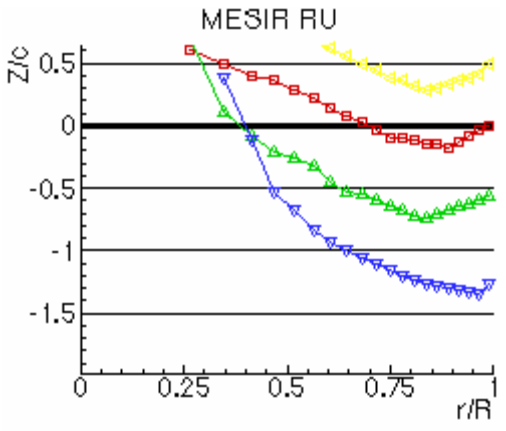

Figure 19 b: Visualization of interaction obliquities in the Z-r plane. (computation performed with MESIR RU)

Evaluation on the Minimum Vibration case

This case corresponds to the same descent conditions as the baseline configuration but High Harmonic Control is applied with the intent to reduce vibrations. For this case we will limit our study to the analysis of the noise footprints. Figure 20 shows a better correlation with the experiment of the BVI noise prediction on the advancing side both in terms of levels and directivity with the MESIR RU wake. The increased intensity of the interaction on the advancing side is due to increased parallelism (X-Y plane). Concerning the retreating side the

prediction is degraded, the MESIR RU wake seems to be too high compared to the experiment, which leads to increased miss distances and a reduction of noise levels. This phenomenon remains to be investigated.

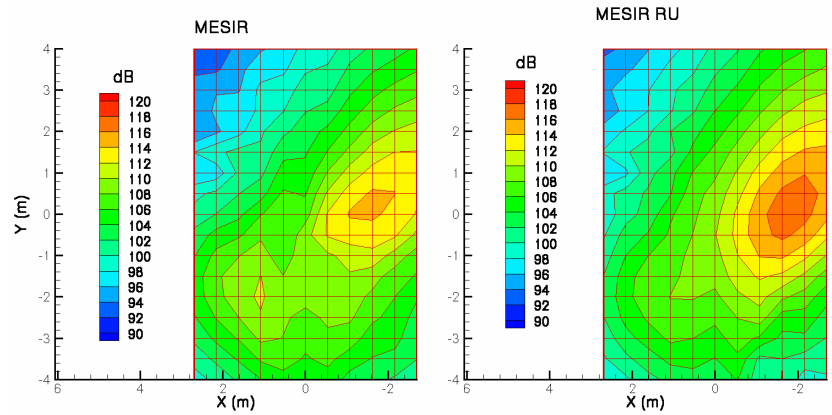

Figure 20 a: HART II Minimum Vibration case. Comparison of noise footprints obtained with MESIR (left) and MESIR RU (right).

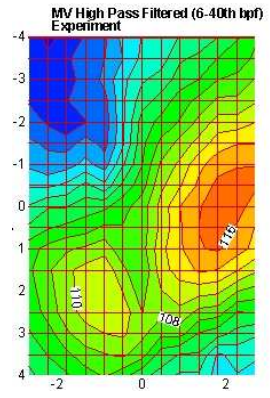

Figure 20 b: HART II Minimum Vibration case. Measured noise footprint

Concept evaluation: concluding remarks

Considering the whole three HART II cases, it can be concluded that several characteristics of the interaction geometries have been ameliorated: parallelism (XY plane), obliquity (Z-r plane), distance between the roll ups generated by successive blades. However this implementation had no positive impact on the vertical positioning of the wake (Figures 15-a and 17-a) and thus on the prediction of the miss distance as we could have expected.

CONCLUSION

This article has presented how a highly instrumented wind tunnel test such as HART II could be used to enhance BVI prediction codes based on a comprehensive analysis approach. Actually a more detailed knowledge of the vortex evolution has lead to significant progresses concerning the empirical laws describing the vortex structure and the aging process. The importance of the vortex parameters (core radius, velocity profile) for an accurate BVI noise prediction has been demonstrated. Another output of HART II, the precise measurements of the wake positions, was then used to assess the concept consisting in including a roll up model in the free wake computation. Putting at equilibrium a rolled up wake has resulted in moderate improvements of the wake geometry and of BVI noise prediction. Following this study, one can consider that these models have reached a degree of completion enabling a reliable BVI noise prediction, which will be used in ONERA future works to design quiet blade geometries or active control devices.

AKNOWLEDGEMENTS

The authors would like to thank Michel Costes for his help concerning MESIR. The authors would also like to acknowledge Gilles Rahier for his scientific advice through the study.

REFERENCES

[1] Makinen, S.M., Hill, M., Gandhi, F., Long, L.N., Vasilescu, R., Sankar, L., "A study of the HART-I Rotor with Loose Computational Fluid/structural Dynamic Coupling", *presented at the 62nd Annual Forum of the American Helicopter Society, Phoenix, AZ, May 2006.*

[2] Gopalan, G., Sitaraman, J., Baeder. J.D., Schmitz, F.H. "Aerodynamic and Aeroacoustic Prediction Methodologies with Application to the HART II Model Rotor", *presented at the 62nd Annual Forum of the American Helicopter Society, Phoenix, AZ, May 2006.*

[3] Sim, B. W-C., Lim, J. W., "Blade-Vortex Interaction (BVI) Noise & Airload Prediction Using Loose Aerodynamic/Structural Coupling", *62nd Annual Forum of the American Helicopter Society, Phoenix, AZ, May 2006.*

[4] Bagai, A., Leishman, J.G., "Rotor Free-Wake Modeling using a Relaxation Technique – Including Comparisons with Experimental Data", *Journal of the American Helicopter Society, Vol. 40, No.2, April 1995.*

[5] Le Bouar, G., Costes, M., Leroy-Chesneau, A., Devinant, P., "Numerical Simulations of Unsteady Aerodynamics of Helicopter Rotor in Manoeuvring Flight Conditions", *Aerospace Science and Technology, Vol. 8, pp. 11-25, 2004.*

[6] Michéa, B., Desopper, A., Costes, M. "Aerodynamic Rotor Loads Prediction Method with Free Wake for Low Speed Descent Flight", *18th European Rotorcraft Forum, Avignon, France, September 1992.*

[7] Rahier, G., Delrieux, Y., "Blade-Vortex Interaction Noise Prediction using a Rotor Wake Roll-Up Model", *Journal of Aircraft, Vol. 34, n° 4, pp. 522-530, (July-August 1997).*

[8] van der Wall, B.G., Burley. C.L., Yu, Y.H., Pengel, K., Beaumier, P., "The HART-II Test – Measurement of Helicopter Rotor Wakes", *Aerospace Science and Technology, Vol. 8, No4, pp.273-284, 2004.*

[9] Yu, Y.H., Tung, C., van der Wall, B.G., Pausder, J., Burley, C.L., Brooks, T., Beaumier, P., Delerieux, Y., Mercker, E., Pengel, K., "The HART-II Test: Rotor Wakes and Aeroacoustics with Higher-Harmonic Pitch Control (HHC) Inputs – The Joint German/French/Dutch/US Project", *58th Annual Forum of the American Helicopter Society, Montreal, Canada, May 2002.*

[10] Beaumier, P., Spiegel, P., "Validation of ONERA Aeroacoustic Prediction Methods for Blade-Vortex Interaction Noise by HART Test Results," *51st Annual Forum of the American Helicopter Society, Ft Worth, TX, May 1995.*

[11] Bailly, J., Delrieux, Y., Beaumier, P., "HART II: Experimental Analysis and Validation of ONERA Methodology for the Prediction of Blade Vortex Interaction", *30th European Rotorcraft Forum, Marseille, France, September 2004.*

[12] Rahier, G., Delrieux, Y., "Influence of Vortex Models on Blade-Vortex Interaction Load and Noise Predictions", *Journal of AHS, Vol. 44-1, pp. 26-33, January 1999.*

[13] Yu, Y.H., Gmelin, B., Heller, H., Philippe, J.J., Mercker, E., Preisser J.S., "HHC Aeroacoustic Rotor Test at the DNW – the Joint German/French/Dutch/US HART Project", *20th European Rotorcraft Forum, Amsterdam, Netherlands, 1994.*

[14] Splettstoesser, W.R., Kube, R., Wagner, W., Seelhorts, U., Boutier, A. Micheli, F., Mercker, E., Pengel, K., "Key Results from a Higher Harmonic Control Aeroacoustic Rotor Test (HART)", *Journal of the American Helicopter Society, January 1997.*

[15] Raffel, M., Richard, H., Ehrenfried, K., van der Wall, B.G., Burley, C.L., Beumier, P., McAlister, K., Pengel, K., "Recording and Evaluation Methods of PIV Investigations on a Helicopter Rotor Model", *Experiments in Fluids, Vol. 36, N° 1, pp. 146-156, 2004.*

[16] Burley, C.L., Brooks, T., van der Wall, B.G., Richards, H., Raffel, M., Beaumier, P., Delrieux, Y., Lim, J.W., Yu, Y.H.,Tung, C., Pengel, K., "Rotor Wake Vortex Definition and Validation from 3-C PIV HART-II Study", *28th European Rotorcraft Forum, Bristol, England, September 2002.*

[17] van der Wall, B.G., Richard, H., "Analysis Methodology for 3C PIV Data", *31th European Rotorcraft Forum, Florence, Italy, September 2005.*

[18] P. Plantin de Hugues., "Etude du système tourbillonaire généré en extrémité de pale d'un rotor d'hélicoptère en stationnaire", *Thèse de Docteur de l'Université d'Aix-Marseille II, 1991.*

[19] Ramasamy, M., Leishman, J.G., "Reynolds Number Based Blade Tip Vortex Model", 61st *Annual Forum of the American Helicopter Society, Grapevine, Texas, June 2005.*

[20] Rahier, G.., "Modelling of airfoil-vortex interaction and application to a helicopter rotor. Contribution to blade-vortex interaction noise prediction", PhD Thesis University of PARIS VI, 1996